# Chemical Peculiarities and Stellar Parameters: A Statistical Study

S. Ghazaryan*[1,2], J. Gómez†[3,4], and G. Alecian‡[5]

[1]Byurakan Astrophysical Observatory, Aragatsotn Province, village Byurakan, 0213, Armenia
[2]A. I. Alikhanyan National Science Laboratory, 2 Alikhanian Br. St., 0036, Yerevan, Armenia
[3]Observatorio Astronómico Ramón María Aller, Universidade de Santiago de Compostela, Av. Das Ciencias, s/n, Campus Vida, Santiago de Compostela, 15782, Galiza, Spain
[4]Departamento de Matemáticas, Universidade de Vigo, Campus Lagoas-Marcosende, 36310 Vigo, España
[5]LUX, Observatoire de Paris, CNRS, Sorbonne Université, PSL, Université, 5 place Jules Janssen, F-92190, Meudon, France

**Abstract**

We investigate the chemical properties of 670 chemically peculiar (CP) stars belonging to seven subclasses: AmFm, ApBp, roAp, HgMn, $\lambda$ Bootis, helium-weak, and helium-rich. The catalog includes 220 stars with abundance measurements published from 2013 to 2025. Using statistical methods, we examine the distribution of elemental abundances and their dependence on effective temperature, surface gravity, projected rotational velocity, and stellar mass. Our analysis demonstrates substantial differences in chemical composition among the subclasses and reveals several statistically significant abundance–parameter relationships. We further explore the role of stellar multiplicity, finding differences in selected chemical abundances and physical parameters between single and non-single objects, single and binary objects. While a detailed statistical analysis will be presented in a forthcoming publication, we include selected results here that were not covered in the final version of the submitted article.

***Keywords:*** *chemically peculiar stars – abundances – statistical analysis*

## 1. Introduction

Chemically peculiar (CP) stars are main-sequence objects exhibiting unusual atmospheric chemical compositions, characterised by significant overabundances or deficiencies of certain elements compared with normal stars of similar spectral types. They comprise several subclasses, including AmFm, ApBp, HgMn, helium-rich, helium-weak, and $\lambda$ Bootis stars (Preston, 1974, Smith, 1996). Their chemical anomalies are generally associated with atomic diffusion, driven by the competition between gravitational settling and radiative acceleration (Michaud, 1970, Michaud et al., 2015). Magnetic fields, rotation, mass loss, and turbulence may also influence the resulting abundance patterns.

To investigate the chemical diversity of these objects, we have progressively developed a database of stellar abundances and fundamental parameters, initially focusing on HgMn stars (Ghazaryan & Alecian, 2016) and subsequently extending it to other CP subclasses (Ghazaryan et al., 2018, 2019, 2021). The increasing availability of high-resolution spectroscopic observations has provided new abundance measurements, motivating a substantial revision of our previous compilations.

In this work, we extend the database with abundance determinations published between 2013 and 2025, incorporating new objects and corrections to the existing catalogue. The resulting sample contains 670 stars from seven CP subclasses, with abundances homogenised to the solar reference scale of Asplund et al. (2009). We analyse the abundance distributions, their relationships with fundamental stellar parameters, and possible differences between single and non-single stars, providing new observational constraints on the chemical properties of CP stars.

*satenikghazarjan@yahoo.de, Corresponding author
†jorge.gomez.crespo@uvigo.gal
‡georges.alecian@obspm.fr

## 2. Data compilation

Our catalogue contains 670 chemically peculiar (CP) stars belonging to seven subclasses: AmFm, ApBp, roAp, HgMn, $\lambda$ Bootis, He-weak, and He-rich. The abundance measurements were collected from 360 published studies, primarily based on high-resolution spectroscopy. Stellar classifications follow the original literature, while the catalogue includes atmospheric parameters ($T_{\rm eff}$, $\log g$, and $v \sin i$) and, when available, additional stellar properties such as mass, luminosity, radius, age, magnetic field strength, and rotational period. The complete catalogue and corresponding references are provided in the online supplementary material.

Abundance measurements from different sources were compiled while preserving the original determinations as far as possible. When multiple ionisation stages were available, their arithmetic mean was adopted, with uncertainties combined following the procedure of Ghazaryan et al. (2018). All abundance measurements were converted to the solar reference scale of Asplund et al. (2009), following our previous compilations (Ghazaryan & Alecian, 2016, Ghazaryan et al., 2018, 2019, 2021). Values given as $N(A)/N_{\rm tot}$ were transformed to the $N(A)/N(H)$ scale by adding 0.0357 to their logarithms. The updated catalogue includes approximately 220 additional stars. Since the original studies employ different atmospheric models and analysis techniques, systematic uncertainties remain and the reported errors should be considered lower limits. Information on stellar multiplicity, including spectroscopic and visual binaries, was collected mainly from SIMBAD (Wenger et al., 2000) and complementary literature.

Figure 1 of our paper sent to MNRAS presents the abundance distribution of all elements included in the updated catalogue, relative to the solar reference abundances.

## 3. Abundances across the CP-star groups

The distributions reveal distinct chemical patterns and substantial star-to-star variations. AmFm stars show considerable scatter among heavy elements, while ApBp and roAp stars exhibit particularly strong enhancements of rare-earth elements, sometimes exceeding 5 dex. HgMn stars display the widest overall abundance range, from significant deficiencies to extreme enhancements, with Hg reaching 6.61 dex. In contrast, $\lambda$ Boo stars are mainly characterised by metal deficiencies, particularly among light and iron-peak elements. He-weak stars combine helium depletion with enhancements of selected heavy elements, whereas He-rich stars show comparatively moderate abundance variations.

These differences reflect the chemical diversity of CP stars and may be associated with the interplay of atomic diffusion, magnetic fields, rotation, and other physical processes. Observational limitations and differences between abundance-analysis methods may also contribute to the observed scatter. The results motivate a statistical examination of the relationships between chemical abundances and stellar parameters.

## 4. Statistical analysis

We applied the non-parametric Kolmogorov–Smirnov (K–S) test Gregory (2005) to compare the abundance distributions of single and multiple CP stars and to examine relationships between elemental abundances and stellar parameters ($T_{\rm eff}$, $\log g$, $v \sin i$, and mass). This test is independent of the underlying distribution and is therefore suitable for our samples Santos et al. (2002). The null hypothesis assumes that both samples originate from the same parent distribution. Two complementary multiplicity analyses were performed. In the first, stars were grouped into single and non-single objects, with binary, cluster stars and higher-order multiple systems combined into a single category. In the second, the multiplicity classes were treated separately, allowing comparisons among single, binary, and multiple systems together with cluster stars. The analysis was carried out for each CP subclass, considering the ApBp and roAp stars jointly, and also separately for single and non-single objects, single and binary objects.

For each element, we calculated the cumulative distribution functions (CDFs) and their maximum difference:

$$D = \sqrt{\frac{n_s + n_m}{n_s n_m}} \max_x |F_s(x) - F_m(x)| \,,$$

where $x$ is the logarithmic abundance, $F_s(x)$ and $F_m(x)$ are the CDFs for single and multiple stars, respectively, and $n_s$ and $n_m$ are the corresponding sample sizes. These sizes vary between elements because


doi: https://doi.org/10.52526/25792776-26.73.2-450

abundance measurements are not available for all stars.

The K–S statistics and corresponding p-values were calculated using Artificial intelligence (AI) tools and are reported in Table 1 and in Table 2. We adopted $p < 0.05$ as the criterion for rejecting the null hypothesis. The statistical analyses were performed in the Google Colab environment (Bisong, 2019).

Preliminary Kolmogorov–Smirnov (K–S) test results reveal statistically significant differences in the abundance distributions of several chemical elements between single and non-single CP stars. An interesting example is shown in Figure 1, which shows the comparative distribution between effective temperature and multiplicity of ApBp and roAp stars. These findings suggest that multiplicity may be an important factor influencing the chemical peculiarity patterns observed in CP stars.

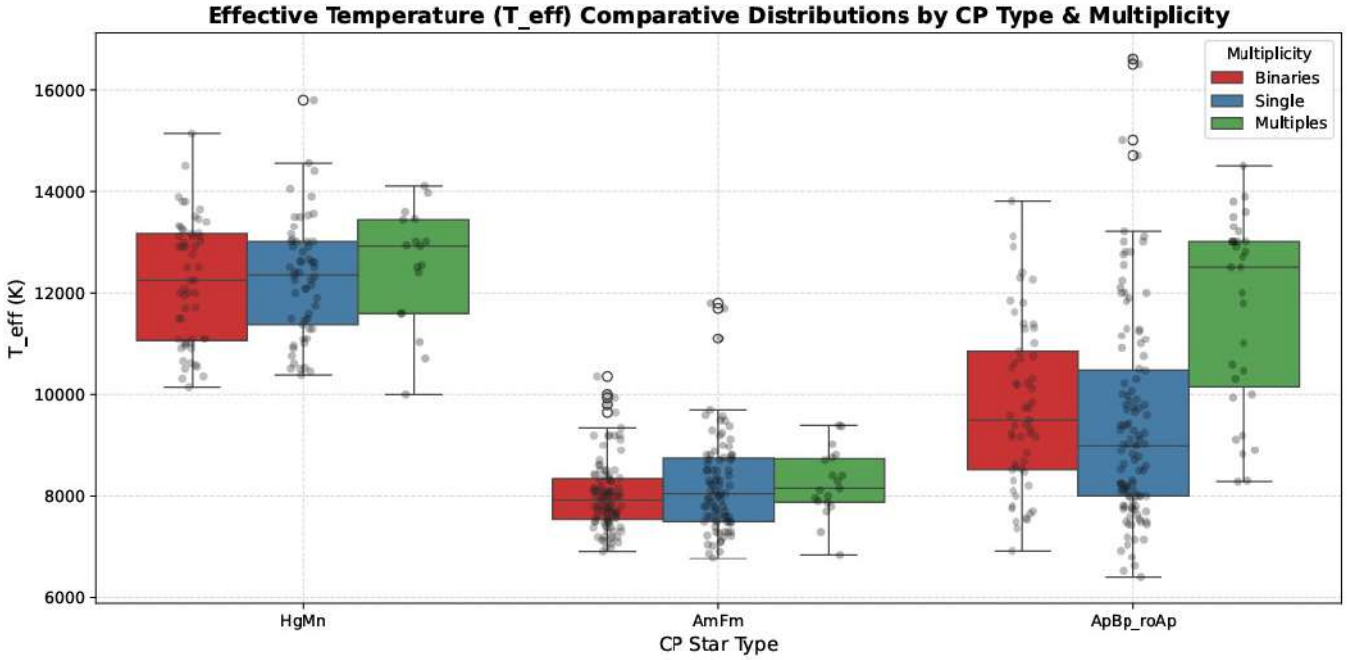


Figure 1: Effective Temperature ($T_{eff}$) Comparative Distributions by CP type and Multiplicity

Table 1: Two-sample Kolmogorov-Smirnov test results comparing **Single** vs **Non-Single** populations across major physical parameters and chemical abundances. Statistically significant differences are shown in boldface ($p \leq 0.05$), while marginal values are underlined ($0.05 < p \leq 0.06$).

| Elements | $T_{\rm eff}$ | | | | $\log g$ | | | | $v \sin i$ | | | | $M$ | | | |
|---|---|---|---|---|---|---|---|---|---|---|---|---|---|---|---|---|
| | $n_1$ | $n_2$ | $D_{\rm esc}$ | $p$ | $n_1$ | $n_2$ | $D_{\rm esc}$ | $p$ | $n_1$ | $n_2$ | $D_{\rm esc}$ | $p$ | $n_1$ | $n_2$ | $D_{\rm esc}$ | $p$ |
| **AmFm stars** | | | | | | | | | | | | | | | | |
| C | 49 | 96 | **0.049** | **0.011** | 49 | 96 | **0.049** | **0.011** | 49 | 96 | **0.049** | **0.011** | 49 | 96 | **0.049** | **0.011** |
| O | 43 | 86 | **0.048** | **0.037** | 43 | 86 | **0.048** | **0.037** | 43 | 86 | **0.048** | **0.037** | 43 | 86 | **0.048** | **0.037** |
| Si | 66 | 106 | **0.038** | **0.014** | 66 | 106 | **0.038** | **0.014** | 66 | 106 | **0.038** | **0.014** | 66 | 106 | **0.038** | **0.014** |
| S | 55 | 70 | **0.056** | **0.004** | 55 | 70 | **0.056** | **0.004** | 55 | 70 | **0.056** | **0.004** | 55 | 70 | **0.056** | **0.004** |
| Cu | 25 | 36 | **0.096** | **0.024** | 25 | 36 | **0.096** | **0.024** | 25 | 36 | **0.096** | **0.024** | 25 | 36 | **0.096** | **0.024** |
| Zn | 42 | 48 | **0.067** | **0.017** | 42 | 48 | **0.067** | **0.017** | 42 | 48 | **0.067** | **0.017** | 42 | 48 | **0.067** | **0.017** |
| Sr | 62 | 62 | **0.052** | **0.008** | 62 | 62 | **0.052** | **0.008** | 62 | 62 | **0.052** | **0.008** | 62 | 62 | **0.052** | **0.008** |
| Y | 57 | 75 | **0.049** | **0.011** | 57 | 75 | **0.049** | **0.011** | 57 | 75 | **0.049** | **0.011** | 57 | 75 | **0.049** | **0.011** |
| Nd | 49 | 49 | 0.054 | 0.056 | 49 | 49 | 0.054 | 0.056 | 49 | 49 | 0.054 | 0.056 | 49 | 49 | 0.054 | 0.056 |
| **ApBp + roAp stars** | | | | | | | | | | | | | | | | |
| Pr | 64 | 48 | **0.062** | **0.005** | 64 | 48 | **0.062** | **0.005** | 64 | 48 | **0.062** | **0.005** | 64 | 48 | **0.062** | **0.005** |
| Nd | 66 | 50 | **0.052** | **0.021** | 66 | 50 | **0.052** | **0.021** | 66 | 50 | **0.052** | **0.021** | 66 | 50 | **0.052** | **0.021** |
| Eu | 59 | 33 | **0.063** | **0.046** | 59 | 33 | **0.063** | **0.046** | 59 | 33 | **0.063** | **0.046** | 59 | 33 | **0.063** | **0.046** |
| **HgMn stars** | | | | | | | | | | | | | | | | |
| He | 26 | 46 | 0.076 | 0.059 | 26 | 46 | 0.076 | 0.059 | 26 | 46 | 0.076 | 0.059 | 26 | 46 | 0.076 | 0.059 |
| Cr | 48 | 54 | **0.054** | **0.041** | 48 | 54 | **0.054** | **0.041** | 48 | 54 | **0.054** | **0.041** | 48 | 54 | **0.054** | **0.041** |
| Y | 32 | 38 | **0.093** | **0.008** | 32 | 38 | **0.093** | **0.008** | 32 | 38 | **0.093** | **0.008** | 32 | 38 | **0.093** | **0.008** |
| **$\lambda$ Boo stars** | | | | | | | | | | | | | | | | |
| Ca | 27 | 28 | 0.092 | 0.059 | 27 | 28 | 0.092 | 0.059 | 27 | 28 | 0.092 | 0.059 | 27 | 28 | 0.092 | 0.059 |
| Ti | 26 | 29 | **0.101** | **0.029** | 26 | 29 | **0.101** | **0.029** | 26 | 29 | **0.101** | **0.029** | 26 | 29 | **0.101** | **0.029** |
| Sr | 16 | 24 | **0.148** | **0.019** | 16 | 24 | **0.148** | **0.019** | 16 | 24 | **0.148** | **0.019** | 16 | 24 | **0.148** | **0.019** |
| **He-rich stars** | | | | | | | | | | | | | | | | |
| N | 15 | 12 | **0.200** | **0.029** | 15 | 12 | **0.200** | **0.029** | 15 | 12 | **0.200** | **0.029** | 15 | 12 | **0.200** | **0.029** |

Table 2: Two-sample Kolmogorov-Smirnov test results comparing **Single** vs **Binaries** populations across major physical parameters and chemical abundances. Statistically significant differences are shown in boldface ($p \leq 0.05$), while marginal values are underlined ($0.05 < p \leq 0.06$).

| Elements | $T_{\rm eff}$ | | | | $\log g$ | | | | $v \sin i$ | | | | $M$ | | | |
|---|---|---|---|---|---|---|---|---|---|---|---|---|---|---|---|---|
| | $n_1$ | $n_2$ | $D_{\rm esc}$ | $p$ | $n_1$ | $n_2$ | $D_{\rm esc}$ | $p$ | $n_1$ | $n_2$ | $D_{\rm esc}$ | $p$ | $n_1$ | $n_2$ | $D_{\rm esc}$ | $p$ |
| **AmFm stars** | | | | | | | | | | | | | | | | |
| C | 49 | 78 | **0.054** | **0.008** | 49 | 78 | **0.054** | **0.008** | 49 | 78 | **0.054** | **0.008** | 49 | 78 | **0.054** | **0.008** |
| O | 43 | 69 | **0.053** | **0.033** | 43 | 69 | **0.053** | **0.033** | 43 | 69 | **0.053** | **0.033** | 43 | 69 | **0.053** | **0.033** |
| Si | 66 | 87 | **0.041** | **0.013** | 66 | 87 | **0.041** | **0.013** | 66 | 87 | **0.041** | **0.013** | 66 | 87 | **0.041** | **0.013** |
| S | 55 | 61 | **0.058** | **0.005** | 55 | 61 | **0.058** | **0.005** | 55 | 61 | **0.058** | **0.005** | 55 | 61 | **0.058** | **0.005** |
| Cu | 25 | 32 | **0.103** | **0.022** | 25 | 32 | **0.103** | **0.022** | 25 | 32 | **0.103** | **0.022** | 25 | 32 | **0.103** | **0.022** |
| Zn | 42 | 40 | **0.069** | **0.030** | 42 | 40 | **0.069** | **0.030** | 42 | 40 | **0.069** | **0.030** | 42 | 40 | **0.069** | **0.030** |
| Sr | 62 | 49 | **0.052** | **0.031** | 62 | 49 | **0.052** | **0.031** | 62 | 49 | **0.052** | **0.031** | 62 | 49 | **0.052** | **0.031** |
| Y | 57 | 59 | **0.047** | **0.041** | 57 | 59 | **0.047** | **0.041** | 57 | 59 | **0.047** | **0.041** | 57 | 59 | **0.047** | **0.041** |
| **ApBp + roAp stars** | | | | | | | | | | | | | | | | |
| Na | 23 | 14 | 0.144 | 0.054 | 23 | 14 | 0.144 | 0.054 | 23 | 14 | 0.144 | 0.054 | 23 | 14 | 0.144 | 0.054 |
| **HgMn stars** | | | | | | | | | | | | | | | | |
| He | 26 | 38 | **0.096** | **0.019** | 26 | 38 | **0.096** | **0.019** | 26 | 38 | **0.096** | **0.019** | 26 | 38 | **0.096** | **0.019** |
| Cr | 48 | 44 | **0.060** | **0.037** | 48 | 44 | **0.060** | **0.037** | 48 | 44 | **0.060** | **0.037** | 48 | 44 | **0.060** | **0.037** |
| Y | 32 | 34 | **0.096** | **0.011** | 32 | 34 | **0.096** | **0.011** | 32 | 34 | **0.096** | **0.011** | 32 | 34 | **0.096** | **0.011** |
| **$\lambda$ Boo stars** | | | | | | | | | | | | | | | | |
| Ca | 27 | 28 | 0.092 | 0.059 | 27 | 28 | 0.092 | 0.059 | 27 | 28 | 0.092 | 0.059 | 27 | 28 | 0.092 | 0.059 |
| Ti | 26 | 29 | **0.101** | **0.029** | 26 | 29 | **0.101** | **0.029** | 26 | 29 | **0.101** | **0.029** | 26 | 29 | **0.101** | **0.029** |
| Sr | 16 | 23 | **0.145** | **0.038** | 16 | 23 | **0.145** | **0.038** | 16 | 23 | **0.145** | **0.038** | 16 | 23 | **0.145** | **0.038** |

## 5. Conclusions

We have presented an updated catalogue of 670 chemically peculiar (CP) stars, including approximately 220 additional objects with abundance determinations published between 2013 and 2025. The catalogue covers seven CP subclasses and incorporates measurements from 360 references, with all abundances homogenised to the solar scale of Asplund et al. (2009).

The abundance distributions reveal distinct chemical patterns among the subclasses. ApBp and roAp stars show pronounced rare-earth element enhancements, HgMn stars exhibit the widest abundance variations, and $\lambda$ Bootis stars are mainly characterised by metal deficiencies. The remaining groups also display characteristic abundance patterns, highlighting the chemical diversity of CP stars.

The statistical analysis identifies significant relationships between elemental abundances and fundamental stellar parameters, although their strengths and directions vary among the subclasses. The Kolmogorov–Smirnov tests also reveal differences in selected abundance distributions and stellar parameters between single and non-single stars, as well as single and binary stars, suggesting that multiplicity should be considered in studies of CP-star chemical properties.

The updated catalogue provides a basis for further investigations of the processes governing chemical peculiarities, particularly the interplay between atomic diffusion, magnetic fields, stellar rotation, and binarity.

Detailed statistical results and the distributions of chemical abundances of different groups of CP stars are discussed in our paper sent to MNRAS.

## Use of Artificial Intelligence Tools

Google Gemini 3.5 Flash (Gemini Team et al., 2024) was used to assist with code organisation, workflow verification, documentation of statistical procedures, and consistency checks. Microsoft Copilot (Microsoft, 2026) was used for language editing and manuscript refinement.

All data analyses, methodological decisions, scientific interpretations, and conclusions were reviewed and approved by the authors, who take full responsibility for the content of this work.

**Acknowledgements**

S. Ghazaryan thanks the RA Higher Education and Science Committee for providing the grant in the framework of the research project № 22RL-039. This work was supported also by the Higher Education and Science Committee of RA (Research project № 24WS-1C001).

# References

Asplund M., Grevesse N., Sauval A. J., Scott P., 2009, Ann. Rev. Astron. Astrophys. , 47, 481

Bisong E., 2019, in , Building Machine Learning and Deep Learning Models on Google Cloud Platform. Apress, Berkeley, CA, pp 59–64, doi:10.1007/978-1-4842-4470-8˙7

Feigelson E. D., Babu G. J., 2012, Modern Statistical Methods for Astronomy, doi:10.48550/arXiv.1205.2064.

Gemini Team Reid M., Savinov N., Teplyashin D., et al., 2024, Gemini 1.5: Unlocking multimodal understanding across millions of tokens of context (arXiv:2403.05530), doi:10.48550/arXiv.2403.05530

Ghazaryan S., Alecian G., 2016, Mon. Not. R. Astron. Soc. , 460, 1912

Ghazaryan S., Alecian G., Hakobyan A. A., 2018, Mon. Not. R. Astron. Soc. , 480, 2953

Ghazaryan S., Alecian G., Hakobyan A. A., 2019, Mon. Not. R. Astron. Soc. , 487, 5922

Ghazaryan S., Alecian G., Paunzen E., Hakobyan A. A., 2021, Communications of the Byurakan Astrophysical Observatory, 68, 517

Gregory P. C., 2005, Bayesian Logical Data Analysis for the Physical Sciences: A Comparative Approach with 'Mathematica' Support

Michaud G., 1970, ApJ, 160, 641

Michaud G., Alecian G., Richer J., 2015, Atomic Diffusion in Stars, Astronomy and Astrophysics Library, Springer International Publishing, Switzerland.

Microsoft 2026, Microsoft Copilot, https://copilot.microsoft.com/

Preston G. W., 1974, Ann. Rev. Astron. Astrophys. , 12, 257

Santos N. C., García López R. J., Israelian G., Mayor M., Rebolo R., García-Gil A., de Taoro M. R. P., Randich S., 2002, Astronomy & Astrophysics, 386, 1028–1038

Smith K. C., 1996, Astrophys. Space. Sci. , 237, 77

Spearman C., 1904, The American Journal of Psychology, 15, 72

Wenger M., et al., 2000, Astron. and Astrophys. Suppl. Ser. , 143, 9